Acta Agriculturae Scandinavica, Section B — Soil & Plant Science

ISSN: 0906-4710 (Print) 1651-1913 (Online) Journal homepage: https://www.tandfonline.com/loi/sagb20

Producing nitrogen (N) uptake maps in winter wheat by combining proximal crop measurements with Sentinel-2 and DMC satellite images in a decision support system for farmers

Mats Söderström, Kristin Piikki, Maria Stenberg, Henrik Stadig & Johan Martinsson

To cite this article: Mats Söderström, Kristin Piikki, Maria Stenberg, Henrik Stadig & Johan Martinsson (2017) Producing nitrogen (N) uptake maps in winter wheat by combining proximal crop measurements with Sentinel-2 and DMC satellite images in a decision support system for farmers, Acta Agriculturae Scandinavica, Section B — Soil & Plant Science, 67:7, 637-650, DOI: 10.1080/09064710.2017.1324044

To link to this article: https://doi.org/10.1080/09064710.2017.1324044

Published online: 08 May 2017.

ACTA AGRICULTURAE SCANDINAVICA, SECTION B — SOIL & PLANT SCIENCE, 2017
VOL. 67, NO. 7, 637–650
https://doi.org/10.1080/09064710.2017.1324044

Producing nitrogen (N) uptake maps in winter wheat by combining proximal crop measurements with Sentinel-2 and DMC satellite images in a decision support system for farmers

Mats Söderström[a], Kristin Piikki[a], Maria Stenberg[b], Henrik Stadig[c] and Johan Martinsson[d]

[a]Department of Soil & Environment, Swedish University of Agricultural Sciences (SLU), Skara, Sweden; [b]Swedish Board of Agriculture, Skara, Sweden; [c]Rural Economy and Agricultural Societies, Skara, Sweden; [d]DataVäxt AB, Hyringa Hedåkers Säteri 3, Grästorp, Sweden

ABSTRACT

Responsive fertilisation of winter wheat (*Triticum aestivum* L.) is often adopted, with N applied two or three times between the developmental stages of tillering and booting. Satellite-based decision support systems (DSS) providing vegetation index maps calculated from satellite data are available to aid farmers in adjusting the topdressing nitrogen (N) rate site-specifically to the current season and to variations in growth conditions within the field. One example is the freely available CropSAT DSS used in Scandinavia, which provides farmers with raster maps of the modified soil-adjusted vegetation index (MSAVI2) calculated mainly from data obtained from satellites Sentinel-2 (ESA, EU) and DMC (DMCii Ltd, Guildford, UK). This study investigated the possibility of calibrating MSAVI2 maps with data from handheld proximal sensor measurements of N uptake covering the main agricultural regions in Sweden during growth stages Z30-45 on the Zadok scale, in order to facilitate farmers' decisions on N rate. More than 200 N-sensor measurements acquired during 2015 and 2016 in seven different winter wheat cultivars were combined with MSAVI2 values from CropSAT. It was found that N uptake could be predicted in a general, national model, i.e. for sites and dates other than those for which the calibration model was parameterised, with a mean absolute error of 11–15 kg N ha^{-1}. A cultivar-specific model performed better than this general model, but a regional model showed no improvement compared with the model parameterised with national data. Vegetation indices calculated from the two narrow bands of Sentinel-2 in the red edge-near infrared region of the crop canopy reflectance spectrum proved to be promising alternatives to the broadband index MSAVI2. Based on the results, we suggest that data from a monitoring programme involving handheld N sensor measurements can be integrated with a satellite-based DSS to upscale N uptake information.

ARTICLE HISTORY
Received 11 February 2017
Accepted 24 April 2017

KEYWORDS
Nitrogen fertilisation; decision support system; remote sensing; proximal sensing; Yara N-Sensor; upscaling; CropSAT; variable-rate application; precision agriculture

Introduction

Winter wheat (*Triticum aestivum* L.) is the most widely cultivated crop in Scandinavia. Split nitrogen (N) fertilisation is commonly adopted to target the economic optimal fertilisation rate and to achieve a desired protein content in the harvested grain. Optimal N fertilisation is also reported to reduce the risk of N leaching (e.g. Lord & Mitchell 1998; Chen et al. 2014; Delin & Stenberg 2014; Basso et al. 2016). Aboveground biomass, leaf chlorophyll concentration and total N content are canopy properties that have been successfully described through the relationship with reflectance in the red and near-infrared (NIR) region of the electromagnetic spectrum (e.g. Jensen et al. 1990; Wiegand et al. 1991; Broge & LeBlanc 2000; Flowers et al. 2003; Gitelson et al. 2003; Reusch 2003, 2005; Tremblay et al. 2009).

Data from satellite images have been used since the mid-1970s to describe and assess the status and vigour of crops (Rouse et al. 1973) and the accessibility and temporal availability of remote sensing imagery is continually improving (Wang et al. 2010; Mulla 2013). During the past two decades a number of commercial systems have been developed in order to support farmers with satellite imagery during the growing season, e.g. Farmsat (Geosys, Morges, Switzerland), Satshot (Fargo, ND, USA), and Farmstar (Airbus Defence and Space, Toulouse, France). However, the use of decision support systems (DSS) for crop production based on optical satellite remote sensing is a challenge in temperate regions frequently covered by clouds such as northern Europe. Broadband indices, such as the normal difference vegetation index (NDVI) (Rouse et al. 1973) and improved

CONTACT Mats Söderström mats.soderstrom@slu.se Department of Soil & Environment, Swedish University of Agricultural Sciences (SLU), Box 234, Skara SE-53223, Sweden

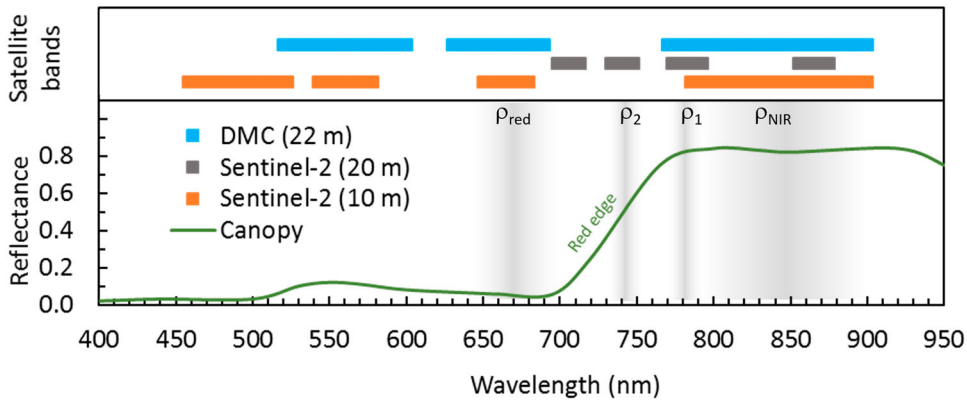

Figure 1. Spectral bands of the satellites used in CropSAT in part of the visible to near-infrared (NIR) region. Common broadband vegetation indices (e.g. NDVI, SAVI, MSAVI2) are based on the reflectance differences in the NIR and red regions (ρ_{RED} and ρ_{NIR}). Combinations of two narrow bands in the red edge-NIR region (ρ_1 and ρ_2) have been reported to be efficient for determination of N uptake (Reusch 2005; Jasper et al. 2009).

versions such as the soil-adjusted vegetation index (SAVI) (Huete 1988) are commonly used to associate the variation in satellite images to properties of the crop (Figure 1). In Scandinavia, a free-to-use, non-commercial DSS based on satellite images (CropSAT), aimed at covering all cropland and assisting farmers in e.g. determining optimal N rate for supplementary fertilisation of winter wheat, has been in use since 2014 (http://cropsat.se; Söderström et al. 2016). In Sweden, CropSAT is funded within a programme for improved nutrient use efficiency and reduced environmental impact (Focus-on-Nutrients) administered by the Swedish Board of Agriculture (Jordbruksverket, Jönköping, Sweden). In Denmark, it is funded by the central advisory organisation (Seges Landbrug & Fødevarer F.m.b.A., Aarhus, Denmark). In the Swedish version of CropSAT, data from the satellites Sentinel-2 (ESA, EU), DMC (the UK-DMC-2 satellite, DMCii Ltd, Guildford, UK) and, to a very limited extent, Landsat 8 (USGS/NASA, USA) are used to calculate a modified version of the soil-adjusted vegetation index (MSAVI2) (Qi et al. 1994):

$$\mathrm{MSAVI2} = \frac{1}{2}[(2 \times \rho\mathrm{NIR} + 1 - \sqrt{[(2 \times \rho\mathrm{NIR} + 1)^2 - 8 \times (\rho\mathrm{NIR} - \rho\mathrm{RED})]} \quad (1)$$

where ρ is reflectance in the red or near infrared (NIR) band (Figure 1). The reason for using MSAVI2 is that initial performance tests indicated that e.g. NDVI reached saturation too early in the season (Söderström et al. 2016). In CropSAT, users can generate MSAVI2 maps over selected agricultural fields. It is then possible to manually assign management actions (e.g. how the supplementary N fertilisation rate should be varied in relation to MSAVI2) and to download prescription files to be used in the fertiliser spreader (Söderström et al. 2016). It is currently recommended that users conduct inspections in different parts of the field with high, medium and low vegetation index, in order to be able to make an appropriate parameterisation of the relationship between the desired application rate and MSAVI2. The N rate at the inspection locations is preferably decided through the use of tools such as a leaf sensor (e.g. the N-Tester (Yara Gmbh, Hanninghof, Germany), which is based on the Minolta SPAD metre and measures light transmitted by the plant leaf at 650 and 940 nm) (Uddling et al. 2007). This can assist in providing an N recommendation to the user. Successful combination of remote sensing data and chlorophyll metres has been reported e.g. by Miao et al. (2009).

To further facilitate the use of satellite data for adjusted N topdressing of small-grain crops at farm level, it would be an advantage if general satellite index maps could be converted to crop properties more relevant in the decision-making process. Extensive comparisons between different combinations of narrow bands (10 nm) for the determination of N uptake in winter wheat have shown that a vegetation index based on two bands in the red edge-NIR region (centred on 730 and 780 nm) is most useful, outperforming e.g. traditional NDVI (Reusch 2005; Jasper et al. 2009). A general vegetation index I (here referred to as ΔRE) was suggested by Reusch (2005):

$$\Delta\mathrm{RE} = \ln(\rho_1) - \ln(\rho_2) \quad (2)$$

where ρ_1 is the reflectance in longest of the two wavebands in the red edge-NIR region. This corresponds well with some 10-nm bands available from the Sentinel-2 satellite (740 and 783 nm, respectively; Figure 1). Various proximal crop sensors that use canopy reflectance have been developed to assess the total N content of the canopy ('N uptake') (e.g. Link et al. 2002; Solie et al. 2002). In Europe,

a commonly used system is the Yara N-Sensor (Yara Gmbh, Hanninghof, Germany), a tractor-mounted proximal sensor that measures reflectance in the visible to NIR spectral range (Link et al. 2002). A handheld version of the instrument also exists and is commonly used in field trials.

To provide farmers with decision support on supplementary topdressing of wheat, handheld Yara N-Sensors are used by different organisations in Sweden (the Swedish Board of Agriculture, the Rural Economy and Agricultural Societies advisory service, Yara AB) in so-called zero plots (field plots with no N fertiliser applied). The N-sensor measurements in these zero plots are used to assess the supply of N from the soil. Measurements are also made in the field adjacent to the plots, where the crop has received N fertiliser according to the farmer's management strategy.

The aim of this study was to combine the latter type of handheld N-Sensor measurements in N fertilised fields with MSAVI2 calculated using data from the satellites Sentinel-2 and DMC in the CropSAT DSS, in order to:

(1) Parameterise prediction models for conversion of MSAVI2 maps to maps of N uptake in winter wheat, calibrated both for all measured cultivars (intended for general use) and for the most common cultivar only, and test whether calibrations for a smaller region improved the predictions.
(2) Validate the performance and robustness of such models by testing them for years, dates and locations not included in the calibration dataset.

The ultimate goal was to improve the functionality of CropSAT DSS, so as to facilitate correct decisions on supplementary N fertilisation. Furthermore, since Sentinel-2 also delivers data from narrow bands in the red edge region, we examined whether better correlations with N uptake could be achieved with the ΔRE index using these bands. However, it was not possible to do this on the entire dataset, since the Sentinel-2 satellite has only been in use since 2016.

Materials and methods

Satellite data

We used MSAVI2 vegetation index maps from the CropSAT DSS from 2015 to 2016. CropSAT was initially primarily based on DMC low-cost data with 22-m spatial resolution, with Landsat 8 data (30-m spatial resolution) as backup. Spectral bands and spatial resolutions of the satellite imagery are presented in Figure 1 and in Table 1. From 2016, data designed for use in vegetation studies, with higher spatial resolution (10 m) and additional spectral bands within the red edge region of the crop canopy spectrum (20-m resolution), became available from the first of two Sentinel-2 satellites (Figure 1). CropSAT covers ~2.4 million ha of arable land in Sweden, i.e. ~90% of arable land in the country (Figure 2). The initial intention with CropSAT was to provide a practically useful set of vegetation index maps during the period for supplementary N fertilisation of small-grain crops (mid-April to mid-June). At least three cloud-free images for each field, well distributed over the acquisition period, was the goal. With the addition of Sentinel-2 data in 2016, >90% of the area covered by CropSAT was covered by at least three useful images, compared with 67% in 2015 (Figure 3), although May 2015 was unusually cloudy and rainy. All MSAVI2 data used in this study were generated by Sentinel-2 or DMC. Images from the following dates were used:

Table 1. Spectral and spatial resolutions of the satellite imagery. NIR = near infrared.

Satellite	Band no	Spectral region	Spatial resolution (m)	Wavelengths (nm)
Sentinel-2	2	Blue	10 m × 10 m	458–523
Sentinel-2	3	Green	10 m × 10 m	543–578
Sentinel-2	4	Red	10 m × 10 m	650–680
Sentinel-2	8	NIR	10 m × 10 m	785–900
Sentinel-2	5	Red edge/NIR	20 m × 20 m	698–713
Sentinel-2	6	Red edge/NIR	20 m × 20 m	733–748
Sentinel-2	7	Red edge/NIR	20 m × 20 m	773–793
Sentinel-2	8a	Red edge/NIR	20 m × 20 m	855–875
DMC	1	Green	22 m × 22 m	520–600
DMC	2	Red	22 m × 22 m	630–690
DMC	3	NIR	22 m × 22 m	770–900

- **DMC 2015**: April (20, 24), May (17, 27, 29), June (1, 11)
- **DMC 2016:** April (20), May (2, 10, 23, 26, 27, 31), June (3)
- **Sentinel-2 2016:** May (6, 9, 13, 21, 28), June (3, 6)

Landsat 8 data were omitted because: (1) they are only occasionally used in the CropSAT system, and (2) the MSAVI2 calculated from Landsat 8 differs to some extent from that calculated from the other two satellites, owing to differences in the width of the spectral bands. Before calculating the vegetation index, the satellite data were converted to reflectance and atmospherically corrected through dark object subtraction (Chavez 1988). Pixels with clouds or cloud shadows were manually removed, as were pixels within 15 m of the field border. Field borders were derived from a spatial database of cultivated arable land (within the EU subsidies database held by the Swedish Board of Agriculture, the so-called 'Block map', version 2015). In the CropSAT DSS, removed pixels along field borders are subsequently recalculated (through averaging) by the remaining, neighbouring pixels within the field. The

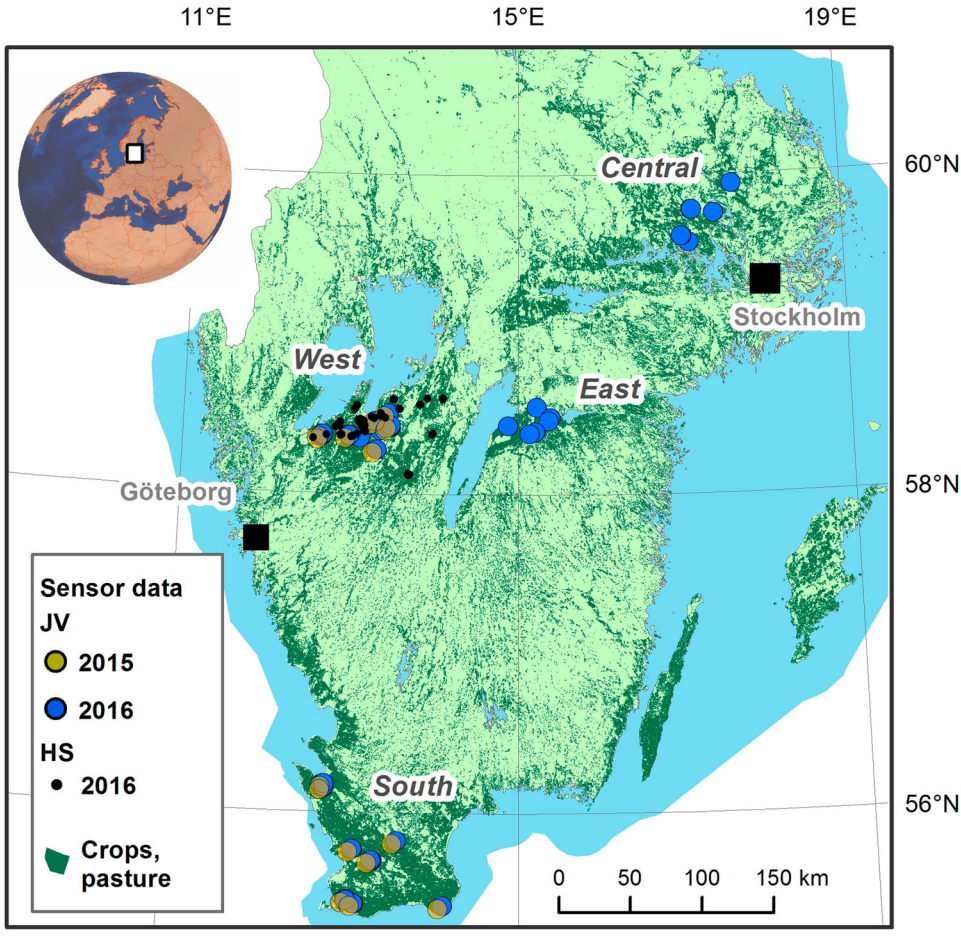

Figure 2. Agricultural areas (dark green) in Sweden covered by satellite data in the CropSAT decision support system. The four regions (South, West, East, Central) and the point locations where reference data were collected by the handheld Yara N-Sensor are shown. The reference data constitute two datasets: JV (collected by the Swedish Board of Agriculture) and HS (collected by the Rural Economy and Agricultural Societies advisory service) (the latter in the West region only). The cities of Stockholm and Gothenburg are shown for orientation purposes only.

images data were processed using ArcGIS 10.3 (Esri Inc. Redlands, CA, USA).

Crop sensor data collected in the field

The handheld Yara N sensor (Yara Gmbh, Hanninghof, Germany) is a portable canopy spectrometer. It registers reflected light from the crop (450–890 nm in 10 nm bands) at an oblique angle (64°). Weekly field measurements (about mid-April to mid-June, targeted to cover the development of winter wheat N uptake through the topdressing period) were conducted in 2015 and 2016 within the advisory service programme Focus-on-Nutrients, a national undertaking for improved nutrient-use efficiency administered by the Swedish Board of Agriculture (locations marked JV in Figure 2). The measurement scheme included measurements in zero plots (i.e. plots not fertilised with N) and measurements in the surrounding field (i.e. in fertilised crop). Only data from the N fertilised fields were used, not from the zero N plots. A site judged representative of the surrounding crop was chosen 25 m from the border of the zero plot in the direction into the field along the crop rows. Four recordings in four different directions were carried out at each site. Treading was avoided in the areas for the recordings. The recordings were calculated into N uptake using an in-house developed calibration model by Yara (Yara Gmbh, Hanninghof, Germany). For 2015, data were available from 26 winter wheat fields in south-west and southern Sweden (regions marked West and South in Figure 2). For 2016, data from 36 sites with winter wheat, also including fields in the East and Central regions (marked in Figure 2) were used. The cultivars were: Julius (SWseed, Lantmännen, Malmö, Sweden; SW), Brons (SW), Norin (SW), Ellvis (Scandinavian Seed, Lidköping, Sweden; Ssd), Mariboss (Ssd), Praktik (Ssd) and Olivin (Ssd), with Julius being the most common. Measurements were made in some additional fields, but those sensor data collection points were considered too close to field boundaries

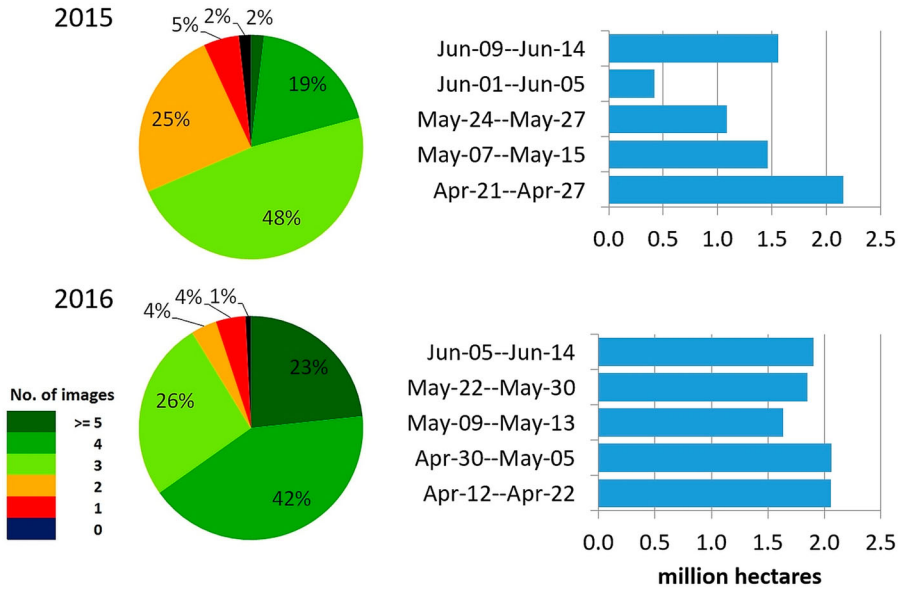

Figure 3. Summary of cloud-free satellite images of arable land in the area displayed in Figure 2. The pie charts to the left show the fraction of arable land area covered with 1, 2, 3, 4 or >5 cloud-free images in the CropSAT decision support system. The column chart to the right shows the area of arable land for which MSAVI2 data were available, summarised for five relatively cloud-free sub-periods of the total period within which CropSAT was run in 2015 and 2016. In reality, there may be more than one image within each of the five sub-periods. (a) All cultivars, tcv validation (ID = i). (b) All cultivars, riv validation (ID = ii). (c) Cv. Julius, tcv validation (ID = iii). (d) Cv. Julius, riv validation (ID = iv).

(<30 m) and were excluded. The Zadok (Z) decimal growth stage (Zadok et al. 1974) during measurement ranged from Z21 to Z57. In this study we included only data collected within Z30–45, i.e. the stages of stem elongation to beginning of booting, which is when most farmers apply N topdressing to winter wheat in Sweden. Coordinates of field measurement locations from 2015 were manually extracted from a general digital map (http://maps.google.com), whereas those from 2016 were positioned by mobile phone GPS (various brands). Both methods resulted in positioning data with some degree of uncertainty, but we assumed that the digital map method was more uncertain than the GPS method. The locations in 2015 were paired with the average vegetation indices of the pixels within a distance of 15–30 m from the coordinates of the sensor measurement, whereas the field data in 2016 were paired with the corresponding satellite image pixels using the GPS coordinates. Field measurements were combined with satellite images if their acquisition dates were within ± 3 days of each other.

In 2016, another set of data (marked HS in Figure 2) collected by the same type of crop sensor was available through the Rural Economy and Agricultural Societies advisory service (Hushållningssällskapet, Skara, Sweden), but only for the West region. These data were collected only once in 50 winter wheat fields during May 23–27 (Z32–39; cv. Julius (SW), Brons (SW), Ellvis (Ssd), Mariboss (Ssd), Praktik (Ssd), Olivin (Ssd) and Reform (R.A.G.T Saaten, Hiddenhausen, Germany; RGT). All datasets collected and used are summarised in Table 2 and the spatial locations are shown in Figure 2.

Table 2. Descriptive statistics on the datasets.

Dataset	*n*	SN [kg N ha^{-1}] (min/median/max)	MSAVI2 [index] (min/median/max)	Z (min/max)	Regions
JV 2015	46	36 / 74 / 110	0.30 / 0.54 / 0.73	30 / 45	S, W
JV 2016	93	12 / 73 / 142	0.26 / 0.52 / 0.75	30 / 45	S, W, E, C
HS 2016	50	17 / 58 / 87	0.14 / 0.43 / 0.60	32 / 39	W

Note: *n* = number of measurements; *SN* = aboveground nitrogen content in the crop (kg N ha^{-1}) according to handheld Yara N-Sensor; *MSAVI2* = modified soil-adjusted vegetation index; *Z* = growth stage; W = west, E = east, S = south, C = central (shown in Figure 2).

N uptake prediction model

The goal of the N uptake model was to assess the potential for N uptake calibration of vegetation index maps, such as those used in the CropSAT DSS, using handheld crop sensors. In particular, we tested the efficiency of prediction models with parameterisations that were either general or specific in terms of geographical region and winter wheat cultivar included. Modelling was done for:

- All regions, all cultivars ($n = 140$)
- One region (W), all cultivars ($n = 49$)
- All regions, one cultivar (Julius; $n = 66$).

- One region (W), one cultivar (Julius; $n = 30$)

Julius was chosen because it was the most common cultivar and the W region was chosen because it was where the HS dataset could be used for additional validation. We parameterised simple linear regression models (Equation 3) in order to predict N uptake from MSAVI2 data:

$$SN = a \times MSAVI2 + b \quad (3)$$

where SN is the above ground nitrogen content in the crop (kg N ha^{-1}) according to handheld Yara N-Sensor, a is the slope parameter and b is the intercept parameter of the univariate linear regression between SN and MSAVI2.

We carried out two types of validations where predictions were compared with observed data:

- An iterative, temporal leave-one-site out cross-validation (tcv) procedure. For each site and instance, predictions were made with models parameterised with a dataset containing only data from the other year and from earlier occasions the same year and only containing data from the other sites (i.e. prediction site excluded).
- An entirely independent regional validation (riv) using the HS dataset. In this case models developed on the JV dataset, both national and regional, were applied on the HS dataset. As in the former procedure, only data from the other year and from earlier occasions the same year were included in the parameterisation dataset.

The validations were designed to ensure that the validation statistics obtained relevantly assessed the performance of the models if applied in a practical system. Any negative predictions were set to zero.

The validation statistics used were: mean absolute error (MAE) (Equation 4), determination coefficient for a linear regression between predictions and measurements (r^2) (Equation 5), and the Nash-Sutcliffe model efficiency (E) (Equation 6), which indicates how well a plot of predicted versus observed values fits the 1:1-line (Nash & Sutcliffe 1970).

$$MAE = \frac{1}{n}\sum |p - o| \quad (4)$$

$$r^2 = 1 - \frac{\sum (o - p)^2}{\sum (o - \bar{o})^2} \quad (5)$$

$$E = 1 - \frac{\sum (o - p_m)^2}{\sum (o - \bar{o})^2} \quad (6)$$

where o are observed values, $\bar{o}$ is average of observations, p are values predicted by a linear regression model between the predicted and observed values, and p_m are values predicted by the different models for SN. Note that Equations 5 and 6 are similar in principle, but with a difference pertaining to usage; r^2 is determined by a statistical model, whereas the p_m values in Equation 6 are outcomes from an applied model. Values of E can therefore be negative.

A pilot test of red edge indices

The potential performance (assessed through correlation) of the ΔRE index (Equation 2) compared with that of MSAVI2 (Equation 1) for prediction of N uptake in winter wheat (growth stage Z30–43; three cultivars: Brons, Ellvis, Julius) was performed by a limited test. This was done using data from the South region only in 2016, since Sentinel-2 data and proximal sensor data for corresponding dates were only available in that region. For comparison, we also tested two other common indices similarly aimed at representing chlorophyll concentration in the canopy using band combinations in the red edge-NIR region (ρ_1 and ρ_2 in Figure 1). These were: the normalised difference red edge index (NDRE) (Equation 7) (e.g. Barnes et al. 2000) and the chlorophyll red edge index ($CI_{red\text{-}edge}$) (Equation 8) (Gitelson et al. 2003):

$$NDRE = \frac{\rho_1 - \rho_2}{\rho_1 + \rho_2} \quad (7)$$

$$CI_{red-edge} = (\rho_1/\rho_2) - 1 \quad (8)$$

All spatial analyses were conducted in ArcGIS (ESRI, Redlands, CA, USA) with the extension Spatial Analyst and the regression modelling was performed using R (R Core Team 2016).

Results

The linear regression modelling revealed that MSAVI2 maps calculated from Sentinel-2 and DMC satellite data were significantly correlated to N uptake in winter wheat (Z30–45) as predicted by the handheld Yara N-Sensor (Table 3). On national level, a crop-specific model for the winter wheat cv. Julius had a somewhat higher coefficient of determination ($r^2 = 0.72$) than the general model that included all seven wheat cultivars ($r^2 = 0.63$). The same was true for the regional models. However, less of the variation in N uptake could be explained by MSAVI2 in the regional models, possibly due to the fact that there was less variation locally.

Validation statistics of the regression models resulting from the different validation approaches (temporal

Table 3. Results of regression analyses of the MSAVI2 vegetation index calculated from satellite data compared with N uptake as recorded by the handheld Yara N-Sensor in the growth stage interval Z30–45. The national models are based on all JV data, whereas the regional models are based only on JV data for the West region (Figure 2).

	National models		Regional models	
	All cv.	cv. Julius	All cv.	cv. Julius
$\hat{a}$ (slope)	203.5 ± 13.14***	205.2 ± 15.93***	188.5 ± 21.80***	219.9 ± 29.67***
$\hat{b}$ (intercept)	−28.90 ± 6.84***	−32.41 ± 8.46***	−31.78 ± 11.17**	−47.54 ± 15.24**
n	140	66	49	30
r^2	0.63	0.72	0.61	0.65

Numbers within brackets are standard error; cv. = cultivar; n = number of observations; $\hat{a}$ and $\hat{b}$ = estimated parameter values ± standard error. Asterisks denote the significance level at which the null hypothesis (that the parameter is equal to zero) was rejected.
***$p < 0.001$, **$p < 0.01$.

cross-validation (tcv) and regional independent validation (riv)) are reported in Table 4. Scatterplots of the validations are shown in Figures 4 and 5. It proved possible to parameterise linear regression models on the MSAVI2 vegetation index maps derived from satellite data and achieve non-biased predictions of N uptake with a MAE of 10–15 kg N ha in the growth stage interval Z30–45, depending on the model. Slightly more accurate predictions were possible for models calibrated and validated only for cv. Julius compared with general models calibrated and validated for a mix of cultivars (Table 4; compare Figure 4a and 4b with Figure 4c and 4d).

Comparing the validation outcomes in Table 4 (validation model ID: i–iv = national models, v–viii = regional models) and Figure 5 (regional models) with Figure 4 (national models), it can be seen that the regional models (West region only; Figure 2) did not perform better, but rather worse, than the national models. This might have been caused by a relatively low number of reference observations regionally and thereby a less robust model, and also less variation in the data regionally compared with the national dataset (as shown by lower MAE in the regional model validations).

There slight differences in the relationships between r^2 and E found between the tcv and riv validation. When the models were applied on the regional HS dataset, there was in general a larger deviation from the 1:1 line (lower E) between observations and predictions, although MAE was lower in the regional validations than in the national validations. The mixture of satellite data from the two satellites DMC and Sentinel-2 did not seem to affect the predictions (Figure 4a and 4c).

As shown in Figure 6, the three vegetation indices based on narrow bands in the red edge-NIR part of the spectrum (ΔRE, $CI_{red\text{-}edge}$ and NDRE) were far better correlated to N uptake measured by proximal handheld Yara N-Sensor ($r^2 = 0.89$; 0.88; 0.85, respectively) than to N uptake based on the MSAVI2 index ($r^2 = 0.61$). There were only small differences between the red edge indices. The data used in this comparison were from the South region only (shown in Figure 2). All three winter wheat cultivars included in this test closely followed the same regression function in the case of the red edge indices (Figure 6b–6d).

Discussion

Provision of satellite-based decision support for N fertilisation in Scandinavia

Satellite data availability

Until recently, no satellite image-based decision support system for practical use aimed at crop management within the growing season was available in Scandinavia (Söderström et al. 2016). However, with increasing numbers of satellites available and decreasing costs and delivery time of data, it is now possible to make

Table 4. Validation statistics for prediction of N uptake in winter wheat from the MSAVI2 vegetation index maps in the growth stage interval Z30–45.

W.wheat cultivars	Calibration region	Validation region	MAE data	MAE strategy	n	MAE (kg N ha^{-1})	r^2	E	ID
All	S/W/E/C	S/W/E/C	JV	tcv	140	15	0.56	0.56	i
		W	HS	riv	50	11	0.56	0.43	ii
Julius	S/W/E/C	S/W/E/C	JV	tcv	66	14	0.63	0.63	iii
		W	HS	riv	23	10	0.65	0.63	iv
All	W	W	JV	tcv	49	14	0.48	0.42	v
		W	HS	riv	50	12	0.56	0.40	vi
Julius	W	W	JV	tcv	30	15	0.47	0.38	vii
		W	HS	riv	23	11	0.65	0.61	viii

Note: Regions: S = South; W = West; E = East; C = Central (Figure 2). Strategy abbreviations: tcv = temporal cross-validation; riv = regional independent validation. ID is identification code for validation models (i–iv = national models, v–viii = regional models).

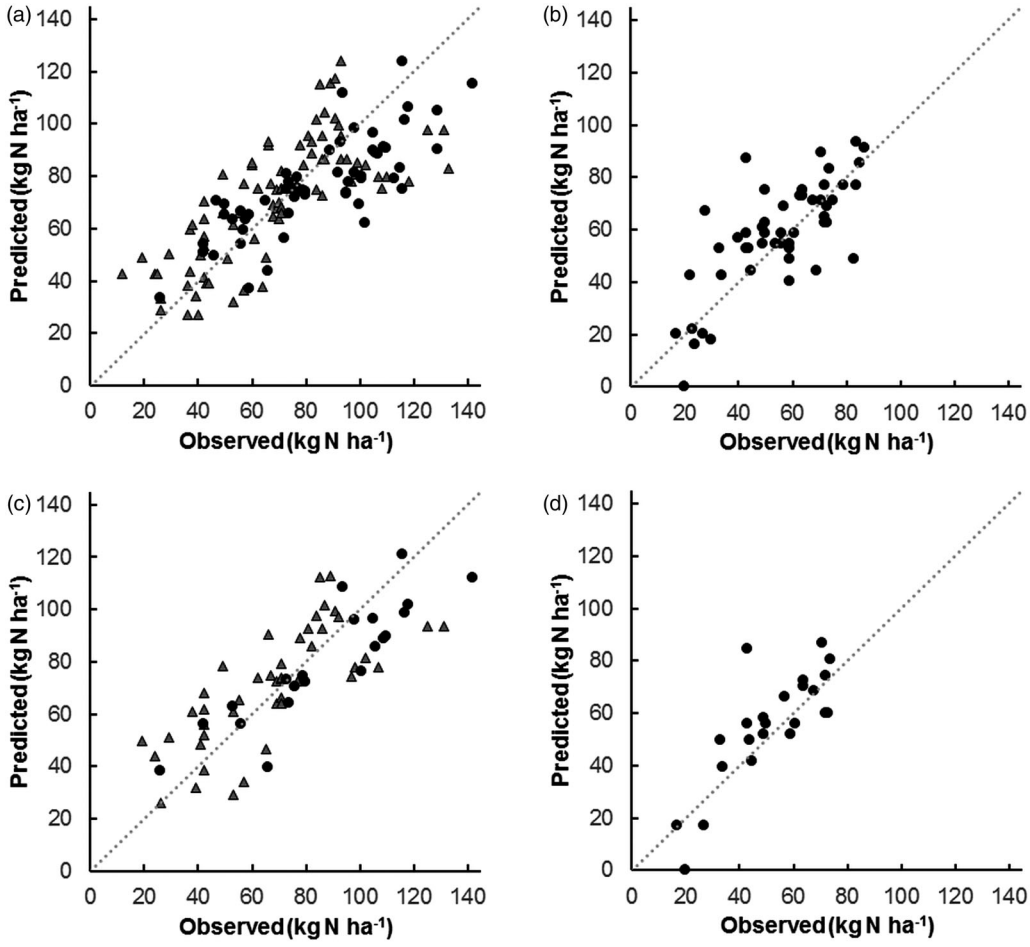

Figure 4. Validation of national (all regions) calibration models for N uptake in winter wheat (cf. Table 4). In (a) and (b) all cultivars (cv.) were used, whereas in (c) and (d) only Julius was used. Validation strategy abbreviations: tcv = temporal cross-validation; riv = regional independent validation (data for the West region only). Triangles are estimates from Sentinel-2 data, dots are estimates from DMC data. (a) All cultivars, tcv validation (ID = v). (b) All cultivars, riv validation (ID = vi). (c) Cv. Julius, tcv validation (ID = vii). (d) Cv. Julius, riv validation (ID = viii).

use of timely remote sensing data for descriptions of crop status on within-field level in Sweden.

Compared with indices based on commonly used broad visible and near-infrared bands, new satellite systems such as Sentinel-2 offer relatively fine resolution (10 m) for a number of bands in the red-edge-NIR region of the electromagnetic reflectance spectrum of a crop canopy. When the second of the Sentinel-2 satellites (2B) becomes operational (planned for 2017), Sentinel-2A and Sentinel-2B in combination might prove sufficient as a free data source for a DSS even in cloudy areas such as northern Europe.

At present, however, with only one Sentinel-2 satellite in operation, relying on data from that satellite would have resulted in lack of cloud-free images for many fields in growth stages Z30-45 (in this case around 10 May to the first week of June), as can be seen in Figure 7. In the sample field shown in Figure 7, only data from the DMC satellite were useful during this period. As shown in Figure 3, most of the arable land in Sweden was covered by cloud-free satellite data several times during the period late April-early to mid-June in 2016. In 2015, when Sentinel-2A data were not available, the coverage was poorer, but this was also due to considerably cloudier conditions in that year. This indicates that even in a cloudy part of the world, such as Scandinavia, it is possible to provide users with free or low-cost data from satellites for use in time-critical applications such as agricultural management.

Stability of spatial variation patterns in crop vigour

The data and workflow overview of the CropSAT DSS are visualised for one 60-ha field in Figure 7, and in that case satellite index maps were available from eight dates in 2016 (between 12 April and 6 June). Farmers and advisors often believe that satellite images must be no more than a few days old if they are to be relevant in portraying crop conditions in fields. This has also been

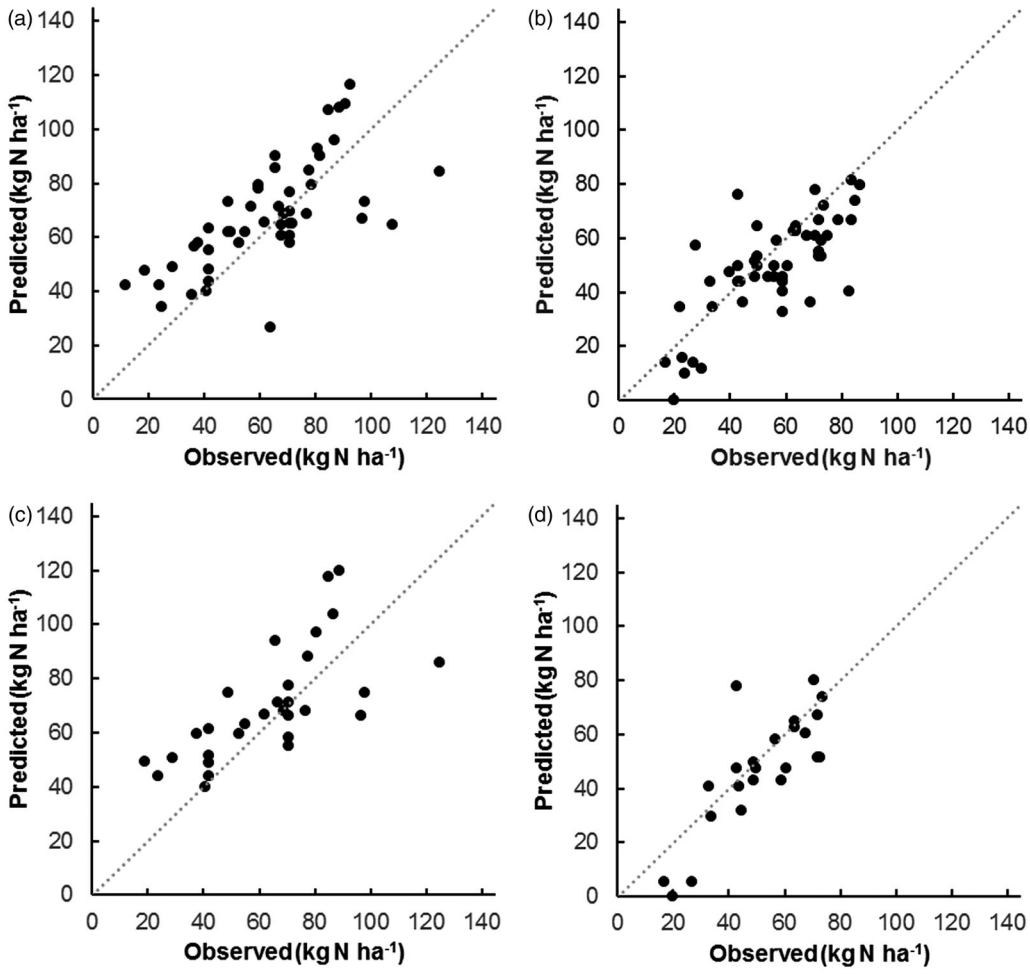

Figure 5. Validation of regional calibration models of N uptake in winter wheat (only West region; Figure 2). In (a) and (b) all cultivars (cv.) were used, whereas in (c) and (d) only cv. Julius was used (see also Table 4). Validation strategy abbreviations: tcv = temporal cross-validation; riv = regional independent validation (the HS-dataset). All estimates based on data from DMC.

reported in the literature (e.g. Muñoz-Huerta et al. 2013). However, experiences from the CropSAT DSS have shown that the within-field spatial pattern of vegetation indices during the period for supplementary fertilisation of small-grain crops is generally relatively stable. In the field in Figure 7, the map shows winter wheat in the southern part and oats (*Avena sativa*, L.) to the north. In addition, the winter wheat area had two different preceding crops, resulting in differences in available soil N, but the spatial pattern was still fairly consistent. This is not an exception (Söderström et al. 2016), and thus the relative variation data in one- to two-week-old vegetation index maps might still be useful as base maps if combined with field calibrations.

Translation of MSAVI2 maps to maps of N uptake

For spatial estimation of the optimal N rate for topdressing, measuring actual N uptake rather than vegetation index values may simplify the process. The results obtained in this study showed that MSAVI2 index maps relatively accurately can be translated to N uptake maps by calibration against proximal N sensor measurements. Even a general national model based on data from two years which included a mix of seven winter wheat cultivars proved useful for within-season prediction of N uptake for growth stage period Z30-45 (validation model *i* in Table 4: $E = 0.56$; MAE = 15 kg N ha^{-1}). The independent regional validation gave lower E and MAE (validation model *ii* in Table 4: $E = 0.43$; MAE = 11 kg N ha^{-1}). The reference dataset used here was somewhat limited, which prevented tests on a range of cultivar-specific models, but a model parameterised specifically for the most common cultivar, Julius, showed some improvements compared with the general model (validation model *iii* in Table 4: $E = 0.63$; MAE 14 kg N ha^{-1}; compare also Figure 4a and 4b with Figure 4c and 4d). This suggests that further and extended proximal sensor measurements for enlarging the reference database would be useful. Therefore we recommend that such

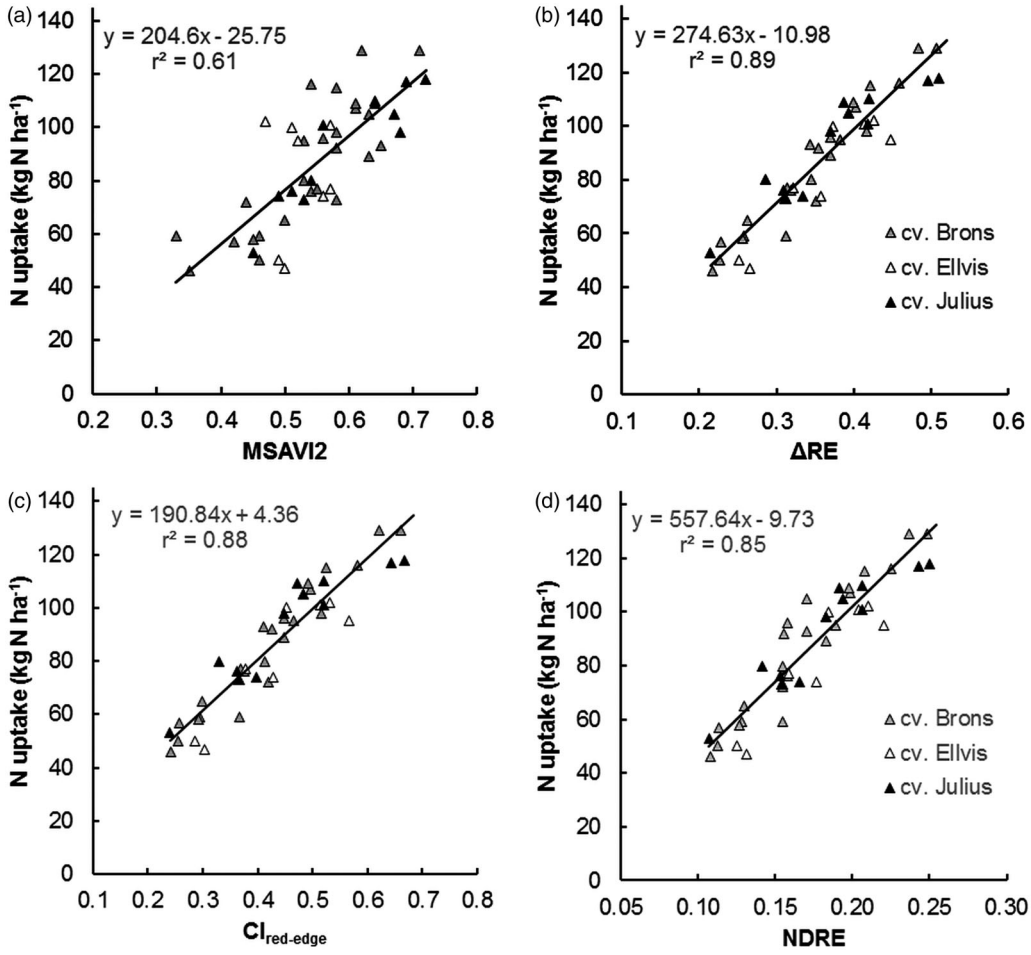

Figure 6. Correlation between N uptake in three cultivars of winter wheat measured by the handheld Yara N-Sensor and (a) MSAVI2, (b) ΔRE, (c) $CI_{red\text{-}edge}$ and (d) NDRE vegetation index calculated from Sentinel-2 data. Growth stage Z30–43, data from the South region only (see Figure 2).

measurements currently conducted throughout the period of N topdressing by the Swedish Board of Agriculture are continued and possibly expanded to include small-grain crops other than winter wheat.

Scope for improvement using sentinel-2 red edge bands

There is scope for improvement of spatial N uptake predictions by using ΔRE or other indices based on bands in the red edge-NIR spectral region, instead of the broad-band index MSAVI2. In the limited test in southern Sweden 2016 reported here (Figure 6), we confirmed findings from e.g. Reusch (2005), who stated that an index based on differences in two bands in the NIR and red edge region (Equation 2) is better related to N uptake in winter wheat than common broad-band indices, here MSAVI2. Combining the narrow 10 nm band 6 (783 nm) and band 5 (740 nm) data from Sentinel-2 in the ΔRE index seems to be a useful alternative to common indices such as MSAVI2 for calibration of Sentinel 2 data against winter wheat N uptake as recorded by the handheld Yara N-Sensor. However, satellite data for narrow bands in this spectral region are still not common. Hence, if a multitude of different satellites are to be combined to improve temporal coverage, then more traditional broad-band indices might be preferred, particularly if assessments of historical data are also of interest.

Improvements through design-based N sensor measurements

There is scope for improvement of spatial N uptake predictions by adopting a design-based N sensor measurement programme aimed at overcoming factors causing noise in the currently used dataset. The noise evident in the validations (Figures 4 and 5) may originate from a number of factors, e.g. variations between cultivars (Reusch 2005) and seasonal differences (Samborski et al. 2009), as well as differences in resolution between the reference data. In this case, the satellite image data had 10×10 m^2 or 22×22 m^2

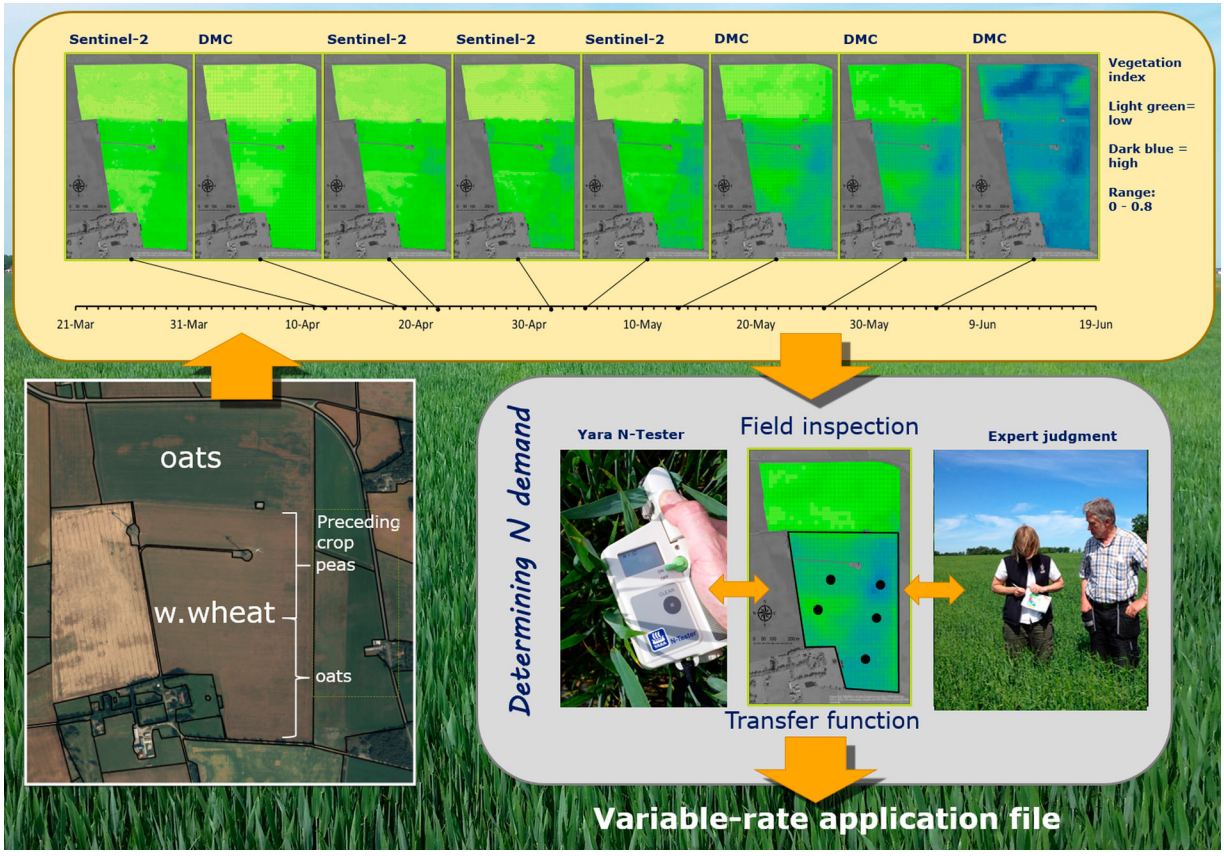

Figure 7. Current working model for the CropSAT satellite image-based DSS used in Scandinavia, exemplified with data for 2016 for one 60-ha field in south-west Sweden. Vegetation index maps are generated from free or low-cost satellite data for most arable fields during the period of supplementary N fertilisation of small-grain crops. Through tools available in the DSS, these maps are manually converted to N application maps based on field inspections, occasionally with the use of low-cost crop sensors. Computer files that control fertiliser spreaders on-the-go can be downloaded. Photo: Christina Lundström.

resolution, while the proximal sensor measurements represented a few square metres. In addition, the positioning of the N sensor measurements was uncertain, especially in 2015, and there was a temporal difference of up to ±3 days in acquisition between proximal sensor data and satellite images. Moreover, atmospheric corrections were made with simple dark object subtraction applied on entire satellite scenes, a rather crude method which does not consider within-scene differences in atmospheric conditions. Despite all these obstacles and pitfalls, application of the models on data from 2015 to 2016 produced reasonable predictions, as shown in the validations (Table 4, Figures 4 and 5). The predicted N uptake was totally out of range (a very low negative prediction which was set to 0) in only one case (in the regional independent validation) (Figure 4b, 4d, 5b and 5d). Data on one particular location with exceptionally low vegetation index resulted in this outlying prediction in all models. Whether this was a result of incorrect positioning of the field-measured data is unknown.

Based on the above, we make the following recommendations for improved calibration data collection:

- Adequate positioning of handheld N sensor measurements (e.g. differential GPS or real-time kinematic GPS).
- Appropriate geographical support of handheld N-sensor measurements for combination with satellite-based raster data, e.g. several sub-readings distributed over a reasonably large area (e.g. 10×10 m^2).
- Collection of sufficient data for parameterisation of cultivar-specific calibration models: at least 20 N-sensor measurements during growth period Z30–Z45 in each of the most common cultivars.
- If possible, synchronisation of handheld N sensor measurements with known satellite passes to reduce time discrepancies between remote and proximal measurements.
- Rapid delivery of collected data for continuous calibration of vegetation index maps to N uptake maps during the season.

Challenges in translating satellite N uptake maps to variable-rate application maps for N

Once N uptake maps are available (e.g. derived by calibration of satellite data), the major remaining challenge is the transfer of spatial N uptake data to decision support for real management actions, for instance prescription files for variable-rate application (VRA). In principle, and irrespective of whether it is determined for an entire field or for a 10×10 m^2 pixel in that field, the N rate to apply depends on the yield potential, the soil N supply, the price ratio between fertiliser N and grain, the amount of N fertiliser applied earlier in the season and whether the goal is to target the economic optimum fertilisation or to achieve a certain protein content. Responsive fertilisation taking the growth conditions of the current year into account is recommended, by splitting the total amount of mineral N into two-three applications. Reference plots with zero fertilisation (indicating soil N supply) can be used as a guide when deciding the N rate in the second and third applications. A drawback of such reference plots is that they are rarely representative of the field average (it is difficult to place them in a representative part of the field) and do not reveal the spatial variation in soil N supply or crop N demand (Samborski et al. 2009). Instead, information on the spatial variation in crop N status can be derived from other tools such as proximal tractor-borne optical sensors or satellite-based DSS. However, there is today no given algorithm for determination of N rate based on either vegetation indices or crop N uptake in growth stage Z30–45. One practical manner in which to apply N uptake maps produced through the models presented in this study could be to first determine a field average N requirement according to common practice (taking the above aspects into consideration), and then redistribute the average N according to the N uptake map. This redistribution need to take into account if other factors than N is expected to limit crop growth, but generally it has been demonstrated that a reasonable approach might be to move N from areas with the lowest and highest values to medium areas (Berntsen et al. 2006), and algorithms built into some tractor-borne N sensors work this way (Söderström et al, 2004). Linear relationships between N uptake and N rate to apply have been reported (Flowers et al. 2003), but these have been found to be highly unreliable and often site-specific (Samborski et al. 2009).

In the satellite-based CropSAT DSS, the transformation of vegetation index maps to N rate maps is done by manual calibration. The user can enter the N rates corresponding to five equally distributed index values and a piecewise linear relationship between N rate and satellite index is fitted. The user is recommended to visit a few sites in the field with different index values (Figure 7) and estimate the optimal rate for N topdressing before performing the manual calibration, either with the help of an N-tester (handheld chlorophyll metre) or through expert judgment and experience. The vegetation index map is then recalculated to an N rate map in a downloadable file that can be used directly for variable-rate application (VRA) by various equipment. Since vegetation indices are relative values reflecting crop vigour, translation to absolute N uptake, as demonstrated here, assists the farmer in decisions on N rates to apply.

Societal value of low-cost or publicly available satellite image-based DSS for VRA for N

An advantage of using satellite data for N management within fields compared with handheld or vehicle-mounted sensors is that the data collected cover huge areas and can be used on a multitude of scales, from watersheds and landscapes to fields. New low-cost or publicly available satellite systems such as Sentinel-2 with high temporal resolution and with additional wavebands targeted for assessment of crop properties opens up exciting possibilities for improved N management and nutrient use efficiency for more efficient food chains.

Easier access to decision support should increase the adoption of VRA for N, which in turn should result in a smaller proportion of arable land being under-fertilised or over-fertilised. Economically optimal nitrogen rate (EONR) has been demonstrated to be a threshold value for increased nitrate leaching (Lord & Mitchell 1998; Delin & Stenberg 2014), and therefore it is important not only from an economic perspective but also from an environmental perspective to avoid N rates higher than EONR.

Summary

We developed empirical relationships between MSAVI2 and N uptake in growth stage Z30–45 based on a combination of satellite data used in an online decision support system and data from handheld crop sensors representing a large part of the arable land in Sweden. The models obtained were evaluated for general use and validated through an iterative, temporal leave-one-field out cross-validation procedure mimicking practical implementation. It proved possible to parameterise linear calibration models for translation of MSAVI2 maps to N uptake maps, resulting in models with MAE ranging between 11–15 kg N ha^{-1}. A cultivar-specific model (cv. Julius) performed better than the general model, but a model calibrated and validated by data

from one region only showed no improvement over the model parameterised with data from all four regions.

The different indices calculated from the two narrow bands of Sentinel-2 in the red edge-NIR spectral region were demonstrated to be promising alternatives to the broadband MSAVI2 index.

Recommendations proposed for continuous hand-held N sensor measurements include collection of sufficient data of suitable quality for parameterisation of cultivar-specific calibrations in order to minimise discrepancies between satellite data and proximal measurements in terms of position, spatial support and time of acquisition.

Disclosure statement

No potential conflict of interest was reported by the authors.

Funding

The development of CropSAT was funded by the Swedish Foundation for Agricultural Research [SLF; project no. H1233115]. Funding for continued development of CropSAT for 2015 and 2016 was provided by the Focus-on-Nutrients programme (Swedish Board of Agriculture), and Agroväst Livsmedel AB, Skara, Sweden. Mary McAfee revised the manuscript linguistically.

Notes on contributors

Mats Söderström is Associate Professor in Soil Science at the Swedish University of Agricultural Sciences (SLU), Skara, Sweden and is an associate member of staff at the International Center for Tropical Agriculture (CIAT), Nairobi, Kenya. His research focuses on applied research in digital soil mapping and precision agriculture often involving proximal and remote sensing of soil and crops.

Kristin Piikki is Associate Professor in Soil Science at the Swedish University of Agricultural Sciences (SLU), Skara, Sweden and is an associate member of staff at the International Center for Tropical Agriculture (CIAT), Nairobi, Kenya. He is active in the research area of precision agriculture and pedometrics and has an avid interest in sustainable intensification of crop production, for example by the development of decision support tools for precision agriculture.

Maria Stenberg is Associate Professor in Soil Science at the Swedish University of Agricultural Sciences (SLU), Skara, Sweden and at the Swedish Board of Agriculture. Her interest is in soil management and efficient use of plant nutrients to mitigate losses to water and air.

Henrik Stadig is Agronomist at the Rural Economy and Agricultural Societies, Skara, Sweden. He provides technical support on precision agricultural techniques to advisors in Sweden and acts as facilitator in the transfer of research results to practical applications.

Johan Martinsson is Business developer at DataVäxt AB (a company that markets software and hardware for precision agriculture and farm management.), Grästorp, Sweden.. He is interested in development of decision support tools for farmers.

References

Barnes EM, Clarke TR, Richards SE, Colaizzi PD, Haberland J, Kostrzewski M, Waller P, Choi C, Riley E, Thompson T, et al. 2000. Coincident detection of crop water stress, nitrogen status and canopy density using ground-based multispectral data. In: Proceedings of the 5th International Conference on Precision Agriculture. Madison, USA: ASA-CSSA-SSSA (published on CD); p. 15.

Basso B, Dumont B, Cammarano D, Pezzuolo A, Marinello F, Sartori L. 2016. Environmental and economic benefits of variable rate nitrogen fertilization in a nitrate vulnerable zone. Sci Total Environ. 545-546:227–235.

Berntsen J, Thomsen A, Schelde K, Hansen OM, Knudsen L, Broge N, Hougaard H, Hørfarter R. 2006. Algorithms for sensor-based redistribution of nitrogen fertilizer in winter wheat. Precis Agric. 7:65–83.

Broge NH, Leblanc E. 2000. Comparing prediction power and stability of broadband and hyperspectral vegetation indices for estimation of green leaf area index and canopy chlorophyll density. Rem Sens Environ. 76:156–172.

Chavez Jr PS. 1988. An improved dark-object subtraction technique for atmospheric scattering correction of multispectral data. Rem Sens Environ. 24:459–479.

Chen X, Cui Z, Fan M, Vitousek P, Zhao M, Ma W, Deng X. 2014. Producing more grain with lower environmental costs. Nature. 514:486–489.

Delin S, Stenberg M. 2014. Effect of nitrogen fertilization on nitrate leaching in relation to grain yield response on loamy sand in Sweden. Eur J Agron. 52:291–296.

Flowers M, Weisz R, Heiniger R. 2003. Quantitative approaches for using color infrared photography for assessing in-season nitrogen status in winter wheat. Agron J. 95:1189–1200.

Gitelson AA, Gritz Y, Merzlyak MN. 2003. Relationships between leaf chlorophyll content and spectral reflectance and algorithms for non-destructive chlorophyll assessment in higher plant leaves. J Plant Phys. 160:271–282.

Huete A. 1988. A soil adjusted vegetation index (SAVI). Rem Sens Environ. 25:295–309.

Jasper J, Reusch S, Link A. 2009. Active sensing of the N status of wheat using optimized wavelength combination: impact of seed rate, variety and growth stage. In: EJ van Henten, D Goense, C Lokhorst, editor. Precision agriculture '09. Wageningen: Wageningen Academic Publishers; p. 23–30.

Jensen A, Lorenzen B, Østergaard HS, Hvelplund EK. 1990. Radiometric estimation of biomass and nitrogen content of barley grown at different nitrogen levels. Int J Rem Sens. 11:1809–1820.

Link A, Panitzk M, Reusch S. 2002. Hydro N-sensor: tractor-mounted remote sensing for variable nitrogen fertilization. In: PC Robert, editor. Proceedings of the 6th International Conference on Precision Agriculture. Madison, USA: ASA/CSSA/SSSA (published on CD); p. 1012–1018.

Lord EI, Mitchell RDJ. 1998. Effect of nitrogen inputs to cereals on nitrate leaching from sandy soils. Soil Use Manage. 14:78–83.

Miao Y, Mulla DJ, Randall GW, Vetsch JA, Vintila R. 2009. Combining chlorophyll meter readings and high spatial resolution remote sensing images for in-season site-specific nitrogen management of corn. Precis Agric. 10:45–62.

Mulla DJ. 2013. Twenty five years of remote sensing in precision agriculture: key advances and remaining knowledge gaps. Biosyst Eng. 114:358–371.

Muñoz-Huerta RF, Guevara-Gonzalez RG, Contreras-Medina LM, Torres-Pacheco I, Prado-Olivarez J, Ocampo-Velazquez RV. 2013. A review of methods for sensing the nitrogen status in plants: advantages, disadvantages and recent advance. Sensors. 13:10823–10843.

Nash JE, Sutcliffe JV. 1970. River flow forecasting through conceptual models part I: a discussion of principles. J Hydrol. 10:282–290.

Qi J, Chehbouni A, Huete AR, Keer YH, Sorooshian S. 1994. A modified soil vegetation adjusted index. Rem Sens Environ. 48:119–126.

R Core Team. 2016. R: A language and environment for statistical computing. Vienna (Austria): R Foundation for Statistical Computing. Available from: http://www.R-project.org/

Reusch S. 2003. Optimisation of oblique-view remote measurement of crop N-uptake under changing irradiance conditions. In: JV Stafford, A Werner, editor. Precision agriculture. Wageningen: Wageningen Academic Publishers; p. 573–578.

Reusch S. 2005. Optimum waveband selection for determining the nitrogen uptake in winter wheat by active remote sensing. In: JV Stafford, A Werner, editor. Precision agriculture '05. Wageningen: Wageningen Academic Publishers; p. 261–266.

Rouse Jr JW, Hass RH, Schell JA, Deering DW. 1973. Monitoring vegetation systems in the Great Plains with ERTS. In: Proceedings Earth Resources Technology Satellite (ERTS) Symposium; 1973 Dec 10–14. 3rd ed. Greenbelt (MD) (Vol. I.) Washington (DC): NASA SP-351, NASA; p. 309–317.

Samborski SM, Tremblay N, Fallon E. 2009. Strategies to make use of plant sensors-based diagnostic information for nitrogen recommendations. Agron J. 101:800–816.

Söderström M, Nissen K, Gustafsson K, Börjesson T, Jonsson A, Wijkmark L. 2004. Swedish farmers' experiences of the Yara N-Sensor 1998-2003. In: Proceedings of the 7th International Conference on Precision Agriculture and Other Precision Resources Management: Hyatt Regency; July 25–28; Minneapolis, USA: International Society of Precision Agriculture; p. 11.

Söderström M, Stadig H, Martinsson J, Piikki K, Stenberg M. 2016. CropSAT – A public satellite-based decision support system for variable-rate nitrogen fertilization in Scandinavia. In: Proceedings of the 13th International Conference on Precision Agriculture (unpaginated, online). Monticello, IL, USA: International Society of Precision Agriculture; p. 8.

Solie JB, Stone ML, Raun WR, Johnson WR, Freeman K, Mullen R, Needham DE, Reed S, Washmon CN. 2002. Real-time sensing and N fertilization with a field scale GreenSeekerTM applicator. In: PC Robert, editor. Proceedings of 6th international conference on precision agriculture. Madison, USA: ASA/CSSA/SSSA (published on CD); p. 1466–1476.

Tremblay N, Wang Z, Ma B-L, Belec C, Vigneault P. 2009. A comparison of crop data measured by two commercial sensors for variable-rate nitrogen application. Precis Agric. 10:145.

Uddling J, Gelang-Alfredsson J, Piikki K, Pleijel H. 2007. Evaluating the relationship between leaf chlorophyll concentration and SPAD-502 chlorophyll meter readings. Photosynth Res. 91:37–46.

Wang K, Franklin SE, Guo X. 2010. The applicability of a small satellite constellation in classification for large-area habitat mapping: a case study of DMC multispectral imagery in west-central Alberta. Can J Rem Sens. 36:671–681.

Wiegand CL, Richardson AJ, Escobar DE, Gerbermann AH. 1991. Vegetation indices in crop assessments. Rem Sens Environ. 35:105–119.

Zadok JC, Chang TT, Konzak CF. 1974. A decimal code for the growth stages of cereals. Weed Res. 14:415–421.